Chinese Chemical Letters 35 (2024) 109137

Contents lists available at ScienceDirect

Chinese Chemical Letters

journal homepage: www.elsevier.com/locate/cclet

Octopus-like DNA nanostructure coupled with graphene oxide enhanced fluorescence anisotropy for hepatitis B virus DNA detection

Jia-Li Xie[a], Tian-Jin Xie[a], Yu-Jie Luo[a], Kai Mao[a], Cheng-Zhi Huang[b], Yuan-Fang Li[a], Shu-Jun Zhen[a,*]

[a] Key Laboratory of Luminescence Analysis and Molecular Sensing (Southwest University), Ministry of Education, College of Chemistry and Chemical Engineering, Southwest University, Chongqing 400715, China
[b] Key Laboratory of Luminescent and Real-Time Analytical Chemistry (Southwest University), Chongqing Science and Technology Bureau, College of Pharmaceutical Sciences, Southwest University, Chongqing 400715, China

ARTICLE INFO

Article history:
Received 11 May 2023
Revised 4 September 2023
Accepted 21 September 2023
Available online 25 September 2023

Keywords:
Fluorescence anisotropy
Graphene oxide (GO)
Octopus-like DNA nanostructure
HBV-DNA

ABSTRACT

Fluorescence Anisotropy (FA) is an effective biochemical detection method based on molecular rotations. Graphene oxide (GO) has been extensively used as an FA amplifier. However, the enhancement of FA by GO alone is limited and the strong scattering of GO will easily make the measurement of FA inaccurate. In order to address these problems, an octopus-like DNA nanostructure (ODN) was designed and coupled with GO to enhance the FA together in this work. By mimicking the multi-clawed structure of the octopus, the ODN can be adsorbed on GO tightly, which not only could improve the sensitivity because of the double FA enhancement abilities of GO and ODN, but also could improve the specificity due to the decrease of the nonspecific interaction in complex samples. Furthermore, ODN could maintain a certain distance between the fluorophore and GO to reduce the fluorescence quenching efficiency of GO, which could improve the accuracy. This method has been applied for the detection of hepatitis B virus DNA (HBV-DNA) in a range of 1–50 nmol/L and the limit of detection (LOD) was 330 pmol/L. In addition, the proposed method has been successfully utilized to detect HBV-DNA in human serum, indicating that this method has a great practical application prospect.

Fluorescence Anisotropy (FA) is a powerful and attractive molecular rotation based method for biosensing [1–4]. At the same time, it is a ratio measurement that reflects intrinsic properties of the fluorophore such as size, rotational diffusion, and lifetime [5,6]. Compared with other fluorescence analysis methods, the FA method is less sensitive to fluorescence fluctuations and photobleaching [7–10]. Up to now, due to the advantages of automated high-throughput capability, homogeneous and accuracy [6,11,12], FA has been widely used to detect various targets including protein [13,14], metal ions [15–18], small molecules [19–23], and nucleic acid molecules [20,24,25]. It is also utilized to explore the interactions between substances [26–29]. However, most methods are limited by the small mass of the targets, leading to limited sensitivities. Therefore, the selection of appropriate FA amplifier is the focus and hotspot of FA research.

Until now, a wide variety of materials have been used as FA signal enhancers, such as proteins [30,31], nucleotides [32,33], and inorganic nanomaterials [22,24,25,34]. Graphene oxide (GO) is a two-dimensional (2D) nanosheet that rotates much slowly than zero-dimensional (0D) spherical nanoparticles with the same surface area, making it an excellent FA amplifier [35,36]. Previously, our research group successfully established a universal detection method for biomolecules by using GO to enhance the FA signal [24]. By indirectly immobilizing the fluorescent dye modified probe DNA on GO through the double-stranded region of its hybridization with a capture DNA fragment that contained poly-A_{20} tail [37–40], the FA value was enhanced and the fluorescence quenching effect of GO was inhibited [41,42]. However, there are still some shortcomings in this method. Firstly, the single poly-A_{20} may leave away from the surface of GO easily because of the competition from biomolecules in complex samples, leading to the decrease of specificity. Secondly, the accumulation of a large amount of double-stranded DNA on GO will lead to the increase of steric effects.

* Corresponding author.
E-mail address: zsj@swu.edu.cn (S.-J. Zhen).

https://doi.org/10.1016/j.cclet.2023.109137
1001-8417/

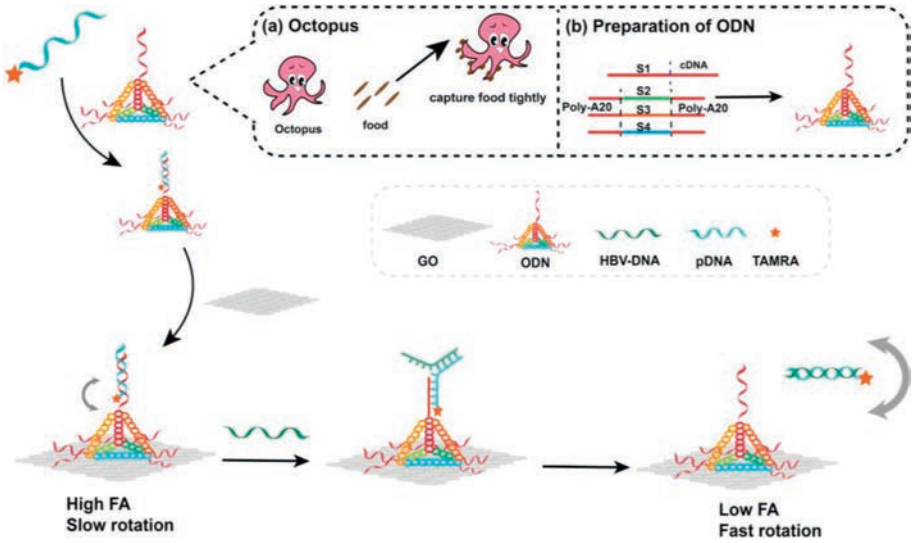

Scheme 1. Illustration of working principle of HBV-DNA detection using ODN-GO amplified FA assay.

Thus, the attack of the target is difficult, which also reduces the detection sensitivity.

In nature, octopus have eight sensitive arms and hundreds of suckers on each arm to catch food tightly [43,44]. Inspired by this natural phenomenon and in order to solve the problems existing in previous GO amplified FA method, we established a new strategy by using GO and octopus-like DNA nanostructure (ODN) to enhance FA together. Herein, DNA tetrahedron was designed to be the body of an octopus, and the six poly-A_{20} extending from the three vertices of the DNA tetrahedron are equivalent to the six claws of the octopus. The six claws were attached tightly to the GO through the π-π stacking [45,46]. At the same time, one of the remaining vertices of the DNA tetrahedron extended a strand of ssDNA, which was set up as the octopus's mouth and paired with a Carboxytetramethylrhodamine (TAMRA) modified probe. Thus, we not only took advantage of the rigid structure of ODN to avoid the fluorescence quenching effect of GO, but also limited the rotation of TAMRA with the large mass (or volume) of ODN and GO to achieve higher FA signal [47,48]. In this work, hepatitis B virus DNA (HBV-DNA) was chosen as a proof-of-concept target. As a common liver virus, HBV is an important cause of liver disease and a threat to human health and public health [49,50]. Therefore, we set up a simple and sensitive FA method to detect HBV-DNA by using the proposed double FA enhancement strategy.

The detection principle was depicted in Scheme 1. The ODN consisted of four oligonucleotides: S1, S2, S3, and S4. Meanwhile, the partial sequence of S1 was designed as capture DNA (cDNA) to hybridize with pDNA, while the rest of oligonucleotides contain the poly-A_{20} to mobilization on the GO. In the absence of HBV-DNA, pDNA hybridized with cDNA on the ODN structure. At the same time, ODN was combined with GO through six poly-A_{20}. Hence, a high FA was observed because the rotation of TAMRA was limited by the GO and ODN, both of which equipped large masses (or volumes). After the addition of HBV-DNA target, the HBV-DNA hybridized with pDNA to form a double-stranded (dsDNA) structure through toehold-mediated strand exchange reaction and left away from the surface of ODN and GO, resulting in a low FA signal on account that TAMRA had a faster rotation rate in solution with small mass of dsDNA. As a consequence, the decreased FA signal was utilized to detect the HBV-DNA.

Firstly, the formation of ODN was confirmed with 12% native polyacrylamide gel electrophoresis (PAGE). ODN was made up of four oligonucleotides in Fig. 1a. The gel images (Fig. 1b) showed

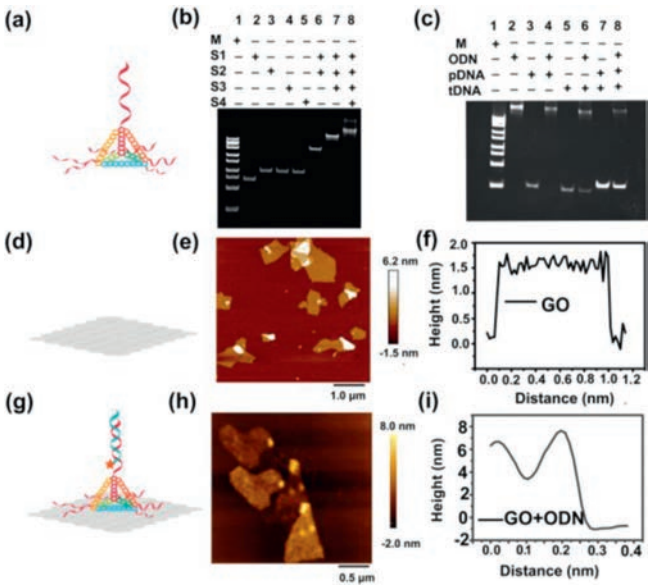

Fig. 1. Characterization of (a-c) ODN, (d-f) GO and (g-i) ODN-GO. (b, c) Image of native PAGE (12%) analysis; M is marker. (e, h) AFM images. (f, i) the height profiles of AFM images.

that the ODN moved more slowly than either the ssDNA or other combinations of ssDNA strands. This result demonstrated that the fabrication of the ODN was successful. In the meantime, it could be clearly found that HBV-DNA could compete with cDNA and formed a dsDNA with pDNA (Fig. 1c). In addition, the GO and ODN-GO structure was characterized by AFM. The experimental results (Figs. 1d-i) showed that the thickness of the ODN-GO complex was larger than that of GO, confirming the successful construction of ODN-GO. At the same time, the successful couple of ODN and GO could also be proved according to the variation of zeta potential in Fig. S1 (Supporting information). As illustrated in Fig. S2 (Supporting information), ODN-GO has good stability within three days of synthesis, and is a stable FA amplification material.

In order to verify the capacity of GO and ODN to enhance FA signal, the FA responses with/without HBV-DNA were investigated. As illustrated in Fig. 2a, the $\Delta r/r_0$ ($\Delta r = r_0 - r$, where r_0 is the FA value in the absence of HBV-DNA, r is the FA value in the presence

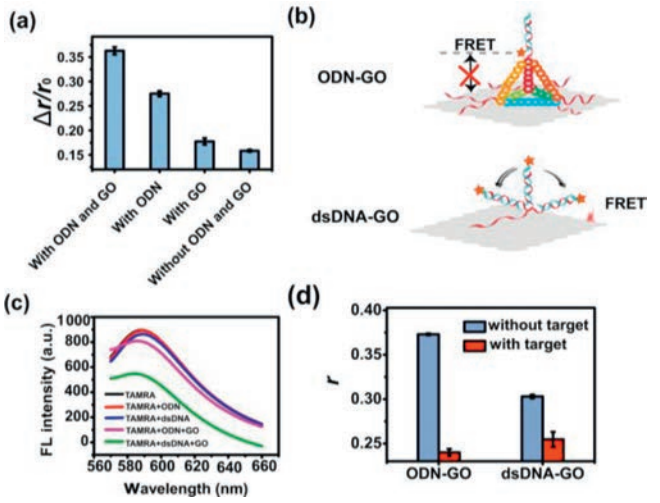

Fig. 2. Feasibility analysis of the strategy. (a) The change of r ($\Delta r/r_0$) induced by HBV-DNA with/without subsequent incubation with GO or ODN. (b) A schematic representation of FA enhancement by the ODN-GO and dsDNA-GO. (c) FL intensity measurements of TAMRA in the absence and presence of cDNA, ODN and GO. (d) Comparison of the responses of the dsDNA-GO and ODN-GO. Each measurement was triplicated (error bars indicate standard deviation). Concentrations: ODN, 50 nmol/L; pDNA, 50 nmol/L; GO, 14.0 μg/mL; HBV-DNA, 40 nmol/L.

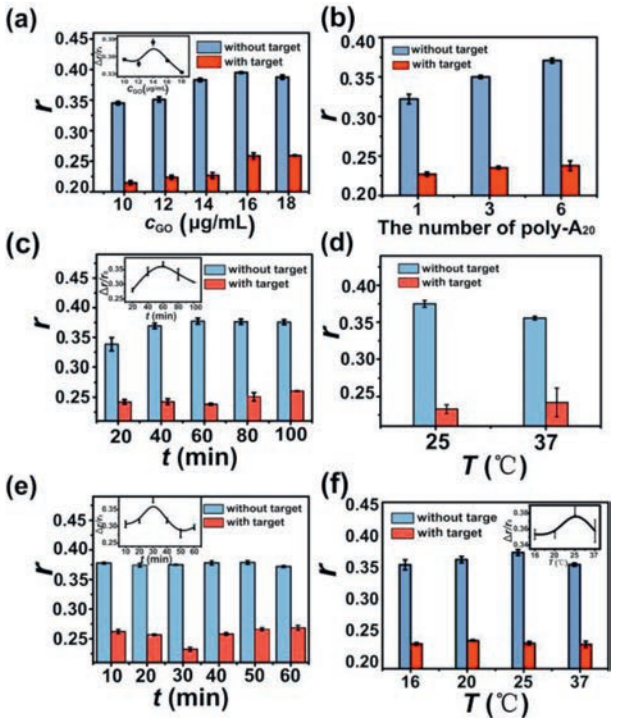

Fig. 3. Optimization of the experimental conditions, including the concentrations of GO (a), the number of poly-A_{20} (b), the incubation times of ODN-GO complex (c), the incubation temperatures of OND-GO complex (d), the reaction times after addition of HBV-DNA (e) and the reaction temperatures after addition of HBV-DNA (f). Each measurement was triplicated (error bars indicate standard deviation). Concentrations: ODN, 50 nmol/L; pDNA, 50 nmol/L; HBV-DNA, 40 nmol/L; GO, 14.0 μg/mL.

of HBV-DNA) was lowest when both GO and ODN did not exist. However, in the presence of GO or ODN, $\Delta r/r_0$ increased slightly. When both GO and ODN existed, the $\Delta r/r_0$ was the highest. The $\Delta r/r_0$ enhanced by ODN-GO was about 2.5 times higher than that of ssDNA alone, and approximately 2 times higher than that of GO alone. Therefore, HBV-DNA could be sensitively detected through the double FA amplification abilities of GO and ODN.

It is well known that GO can quench the fluorescence of fluorophore strongly through fluorescence resonance energy transfer (FRET), which will reduce the accuracy of FA measurement. Therefore, we previously designed a new strategy to immobilize TAMRA modified probe DNA on GO indirectly through the double-stranded region of its hybridization with a capture DNA. However, the double-stranded DNA (dsDNA) was just supported by one poly-A_{20} tail and the ds-DNA could swing on the surface of GO, which would shorten the distance between TAMRA and GO and result in the fluorescence quenching through FRET (Fig. 2b). As shown in Fig. 2c, the fluorescence of TAMRA was quenched by GO obviously even when the length of dsDNA was as long as 7.3 nm. In contrast, although the distance between TAMRA and GO was only about 5.4 nm in the presence of ODN, the fluorescence quenching ability of GO toward TAMRA was inhibited strongly. This phenomenon could be ascribed to the more rigid structure of ODN than dsDNA, which enables the cDNA hybridization fragment on ODN to stand upright. Thus, there was a fixed distance between TAMRA and GO and avoid the FRET process between TAMRA and GO. Therefore, ODN could improve the accuracy of FA measurement. Meanwhile, ODN-GO will have higher sensitivity than dsDNA-GO because the consistent favorable orientation of ODN avoids the possible space crowding and electrostatic interaction [51]. At the same time, we compared the FA enhancement ability of ODN-GO and dsDNA-GO, and the experimental results (Fig. 2d) showed that the ODN-GO had a stronger capacity to enhance FA. That's because the mass (volume) of the ODN was much larger than that of dsDNA, which greatly limited the motion of the TAMRA and improved the sensitivity for target detection.

A series of experimental conditions involved in this study were investigated to obtain the optimal performance for HBV-DNA detection. Firstly, we investigated the effect of the concentration of PBS buffer on the fluorescence intensity and r value of TAMRA modified on pDNA. As shown in Fig. S3 (Supporting information), under different buffering concentration, the fluorescence intensity and fluorescence anisotropy value of TAMRA are unchanged, indicating that the buffer concentration has no effect on this work. However, the hybridization of DNA requires a certain ion concentration, so the PBS concentration we selected in our work is 1 ×. Then, the influence of the concentration of GO on the experiment were explored. If the concentration of GO is too low, only a few ODN will be adsorbed on GO, so the background signal of FA is low. Nevertheless, if the concentration of GO is too high, the FA values is easily affected by light scattering, resulting in reduced accuracy. As shown in Fig. 3a, the value of $\Delta r/r_0$ reached to maximum when the concentration of GO was 14 μg/mL.

Next, we analyzed the influence of the number of poly-A_{20} claws of ODN on the detection signal. If the number of poly-A_{20} claw is small, the ODN could not be adsorbed on GO tightly, which will reduce the detection signal. The experimental results confirmed that the more the poly-A_{20} claws, the greater the r value (Fig. 3b). Therefore, the ODN with six poly-A_{20} claws was utilized for the following experiments.

Furthermore, the influences of the temperature and reaction time of ODN and GO were investigated. With the extension of reaction time, $\Delta r/r_0$ first increased and then reached its maximum value at 60 min (Fig. 3c). When reaction time was too short, the "claws" of ODN did not have time to fix tightly on GO. Instead, when the reaction time became longer, GO would aggregate, resulting in small Δr because of the strong scattering effect. Fig. 3d showed that the optimal reaction temperature of ODN and GO was 25 °C, rather than 37 °C. Hence, lower temperature was more beneficial for GO to adsorb ssDNA.

Besides, the reaction temperature and time after addition of HBV-DNA were also important factors. The experimental results

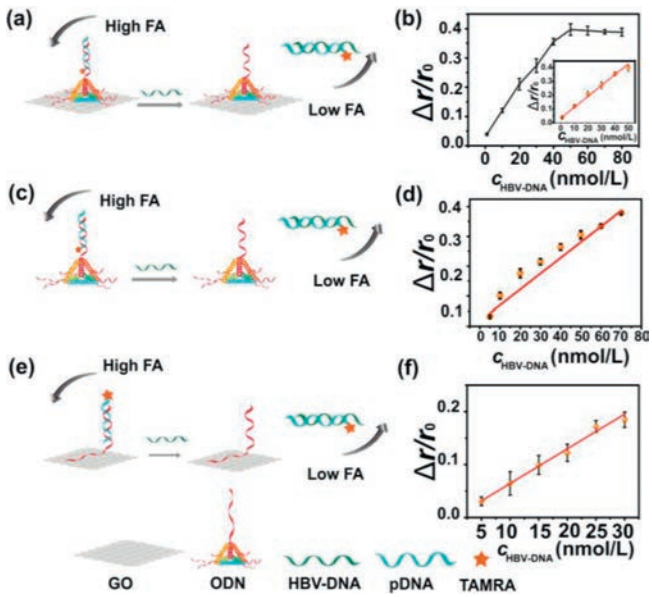

Fig. 4. Comparation of the sensitivities of different FA amplification strategies. (a) Schematics for ODN and GO amplified FA strategy. (b) The linear relationship between $\Delta r/r_0$ and HBV-DNA concentration with the double amplification effect of ODN and GO. (c) Schematics for ODN amplified FA strategy. (d) The linear relationship of between $\Delta r/r_0$ and HBV-DNA concentration with the amplification effect of ODN. (e) Schematics for GO amplified FA strategy. (f) The linear relationship of between $\Delta r/r_0$ and HBV-DNA concentration with the amplification effect of GO. Concentrations: ODN, 50 nmol/L; pDNA, 50 nmol/L; HBV-DNA, 40 nmol/L; GO, 14.0 μg/mL.

(Fig. 3e) showed that when the reaction time of the HBV-DNA was 30 min, $\Delta r/r_0$ reached its maximum value. When reaction time was too short, HBV-DNA did not have time to fully compete with cDNA, and partial pDNA still bound with ODN-GO, inducing a high FA after the addition of the target. Similarly, if reaction time is too long, part of the HBV-DNA will be adsorbed on the surface of GO through π-π stacking, which means that the actual HBV-DNA to hybridize with pDNA is less than the amount of the added target, so the FA value will be reduced. As a consequence, there was not enough HBV-DNA to form a double-stranded structure with pDNA to produce a low fluorescence anisotropy value. At the same time, the optimum reaction temperature was 25 °C (Fig. 3f). When the temperature is lower than room temperature, the rate of DNA chain replacement reaction is low, so the r value is still large after adding the target, resulting in small Δr. On the contrary, when the reaction temperature is higher than room temperature, it is not conducive to the adsorption of ODN on GO, resulting in a decrease in Δr.

In order to verify whether the proposed method can be used for quantitative detection of HBV-DNA, FA responses of HBV-DNA at different concentrations under optimized experimental condition were measured. The schematic diagram of detecting HBV-DNA by ODN and GO dual signal amplification was shown in Fig. 4a. As shown in Fig. 4b, there was a good linear relationship between $\Delta r/r_0$ and HBV concentrations in the range of 1–50 nmol/L. The linear regression equation was $\Delta r/r_0 = 0.008c + 0.033$ (correlation coefficient, $R^2 = 0.99$), where c was the concentration of HBV-DNA (nmol/L). The limit of detection (LOD) was evaluated to be 330 pmol/L ($3\sigma/k$), which was about 14 times lower than our previous work. In comparison of HBV-DNA detection between our work and some reported work, ODN-GO exhibited better sensitivity toward HBV-DNA (Table S2 in Supporting information). Meanwhile, FA responses at different concentrations of HBV-DNA without GO were investigated in Fig. 4c. As shown in Fig. 4d, the linear relationship between the change of FA and HBV-DNA concentration was over the range of 5–70 nmol/L. The linear regression equation was $\Delta r/r_0 = 0.005c + 0.017$ (correlation coefficient, $R^2 = 0.98$) and the LOD was 3.1 nmol/L. In addition, in Fig. 4e, we also compared the detection of HBV-DNA without ODN. As illustrated in Fig. 4f, the LOD was 4.8 nmol/L without ODN, and the linear regression equation was $\Delta r/r_0 = 0.007c + 0.013$ (correlation coefficient, $R^2 = 0.98$). Obviously, the proposed method had improved sensitivity because of the double FA amplification abilities of both GO and ODN.

Table 1
Detection of HBV-DNA in human serum samples ($n = 3$).

Sample	Add (nmol/L)	Found (nmol/L)	Recovery (%)	RSD (%) ($n = 3$)
Human serum	1	0.97 ± 0.2	95.5–99.8	0.2
	5	5.1 ± 0.3	96.8–104	4.1
	10	11.7 ± 0.3	116.4–117.7	0.3
	20	22.3 ± 1	96.6–116	4.5
	40	37.5 ± 2	89–100	6.1

Besides, to investigate the selectivity of this approach, we tested five nucleotides with various sequences, including HBV-DNA, one-base-mismatched (mis-1), two-base-mismatched (mis-2), three-base-mismatched (mis-3) and random sequences (rs) under the same experimental conditions. The results showed in Fig. 5a that the FA response was maximal only in the presence of HBV-DNA. Even if there was only one base mismatch, $\Delta r/r_0$ was only about 1/5 of the FA change induced by the HBV-DNA. Consequently, it was shown that a very precise binding interaction exists between ODN-GO and HBV-DNA. Furthermore, we investigated how this method responded to the interfering substances in human serum because it contains a variety of interfering proteins and ions that can affect *in vitro* diagnostics. As illustrated in Fig. 5b, after the addition of different metal ions and other small molecules substances to the HBV-DNA solutions, the FA responses were almost the same as that of the FA response after the addition of HBV-DNA. We also investigated the influence of common proteins in human serum on the analytical performance of this method. The experimental results indicated that none of these interference substances induced obvious signal changes (Fig. S4 in Supporting information). Therefore, it indicated that the proposed method could effectively resist the interference of complex coexisting components and could be applied to accurately detect HBV-DNA in human serum.

A spike-recovery experiment was carried out by examining the recoveries of HBV-DNA spiked in human serum samples in order to confirm the viability of the proposed approach in real sample detection. Human serum samples were acquired from Southwest University Hospital and strictly abide by the ethics standards of Southwest University Committee (No. yxy2021127). We got informed consents from the blood donor volunteers of this work. The experimental results (Table 1) showed an excellent recovery rate and RSD of HBV-DNA at various concentration levels. In addition, we investigated a spike-recovery experiments only using ODN as an FA amplification material (Table S2). The experimental results show that the recovery rate only in the presence of ODN was poorer and the RSD was larger than that in the presence of ODN-GO, indicating that the ODN-GO has the capacity to accurately detect HBV-DNA in real biological samples.

In summary, ODN and GO were utilized to enhance FA to detect HBV-DNA in this work. Compared with the previous GO amplified FA method, this paper uses ODN to connect fluorescent molecules and GO instead of double stranded DNA. There are several unique features of this design. Firstly, this method has improved sensitivity because both GO and ODN has large mass (or volume). Secondly, ODN is more rigid than double stranded DNA, which en-

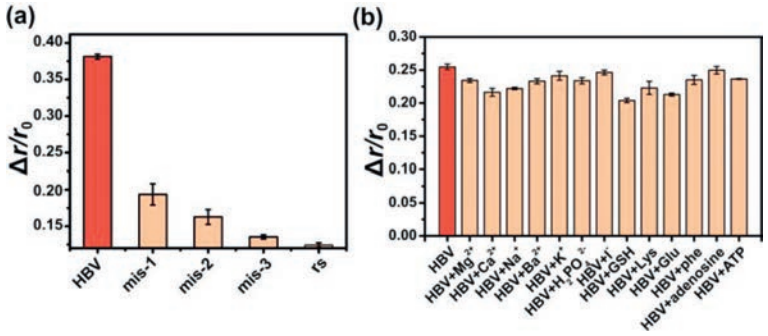

Fig. 5. (a) Selectivity of the proposed method. Concentrations: ODN, 50 nmol/L; pDNA, 50 nmol/L; HBV-DNA, 40 nmol/L; GO, 14.0 μg/mL. (b) The anti-interference property of the proposed method. Each measurement was triplicated (error bars indicate standard deviation). Concentrations: ODN, 50 nmol/L; pDNA, 50 nmol/L; HBV-DNA, 30 nmol/L; GO, 14.0 μg/mL.

sures a certain distance between fluorescent molecules and GO and improves the accuracy of detection. Thirdly, six poly-A_{20} claws of ODN can be adsorbed on GO together, which can make ODN firmly coupled with GO in complex biological environment to improve the anti-interference ability of this method. Besides, when a large number of ODNs are stacked on the GO surface, the steric hindrance of HBV-DNA to compete with cDNA decreases due to the large volume of ODN, and the reaction efficiency is improved. Given these advantages, we believe that our proposed method can be used as a routine tool for biomolecular analysis in biomedical and molecular disease diagnosis in future.

Declaration of competing interest

The authors declare that they have no known competing financial interests or personal relationships that could have appeared to influence the work reported in this paper.

Acknowledgments

This work was supported by the National Natural Science Foundation of China (Nos. 21974109, 22322409), the Natural Science Foundation of Chongqing (No. CSTB2022NSCQ-MSX1662), and the Fundamental Research Funds for the Central Universities (No. XDJK2019TY003).

Supplementary materials

Supplementary material associated with this article can be found, in the online version, at doi:10.1016/j.cclet.2023.109137.

References

[1] D. Zhang, M. Lu, H. Wang, J. Am. Chem. Soc. 133 (2011) 9188–9191.
[2] X. Xiao, S. Zhen, RSC Adv. 12 (2022) 6364–6376.
[3] K. Chullipalliyalil, K. Elkassas, M.A.P. McAuliffe, S. Vucen, A. Crean, Anal. Chem. 95 (2023) 2774–2782.
[4] D. Zhang, H. Wang, Anal. Chem. 91 (2019) 14538–14544.
[5] W. Huang, C. Guo, J. Zhai, X. Xie, Anal. Chem. 94 (2022) 9793–9800.
[6] Q. Huang, B. Chen, J. Shen, et al., J. Am. Chem. Soc. 143 (2021) 10735–10742.
[7] J. Chen, J. Liu, X. Chen, H. Qiu, Chin. Chem. Lett. 30 (2019) 1575–1580.
[8] S. Jain, A. Heiser, A.R. Venter, Analyst 136 (2011) 1298–1301.
[9] T.L. Mann, U.J. Krull, Analyst 128 (2003) 313–317.
[10] Y.L. Fan, Z.Y. Liu, Y.M. Zeng, et al., Talanta 223 (2021) 121721.
[11] B. Yang, X.B. Zhang, L.P. Kang, et al., Anal. Chem. 85 (2013) 11518–11523.
[12] C. Zeng, J. Gao, Y. Lou, L. Cui, Talanta 218 (2020) 121179.
[13] M. Zou, Y. Chen, X. Xu, et al., Biosens. Bioelectron. 32 (2012) 148–154.
[14] A. Pepanian, P. Sommerfeld, R. Kasprzyk, et al., Anal. Chem. 94 (2022) 14410–14418.
[15] B.C. Yin, P. Zuo, H. Huo, X. Zhong, B.C. Ye, Anal. Biochem. 401 (2010) 47–52.
[16] Y. Yu, Y. Liu, S.J. Zhen, C.Z. Huang, Chem. Commun. 49 (2013) 1942–1944.
[17] B.C. Ye, B.C. Yin, Angew. Chem. Int. Ed. 47 (2008) 8386–8389.
[18] J. Zhang, J. Tian, Y. He, Y. Zhao, S. Zhao, Chem. Commun. 50 (2014) 2049–2051.
[19] X. Xiao, J. Tao, H.Z. Zhang, C.Z. Huang, S.J. Zhen, Biosens. Bioelectron. 85 (2016) 822–827.
[20] Y.X. Liu, X. Xiao, C.H. Li, et al., Talanta 211 (2020) 120730.
[21] Q. Zhao, Q. Lv, H. Wang, Anal. Chem. 86 (2014) 1238–1245.
[22] Y. Li, H. Yu, Q. Zhao, RSC Adv. 12 (2022) 7464–7468.
[23] C. Hoffmann, M. Jourdain, A. Grandjean, A. Titz, G. Jung, Anal. Chem. 94 (2022) 6112–6119.
[24] X. Xiao, Y.F. Li, C.Z. Huang, S.J. Zhen, Chem. Commun. 51 (2015) 16080–16083.
[25] S.J. Zhen, X. Xiao, C.H. Li, C.Z. Huang, Anal. Chem. 89 (2017) 8766–8771.
[26] B. Billet, B. Chovelon, E. Fiore, et al., Angew. Chem. Int. Ed. 60 (2021) 12346–12350.
[27] L. Gao, L. Liu, Y. Tian, et al., Anal. Chem. 93 (2021) 7045–7053.
[28] E. Sijbesma, B.A. Somsen, G.P. Miley, et al., ACS Chem. Biol. 15 (2020) 3143–3148.
[29] Q.H. Wan, X.C. Le, Anal. Chem. 72 (2000) 5583–5589.
[30] Y. Li, L. Sun, Q. Zhao, Talanta 174 (2017) 7–13.
[31] Y. Li, Q. Zhao, Anal. Chem. 91 (2019) 7379–7384.
[32] Z. Zhu, T. Schmidt, M. Mahrous, et al., Anal. Chim. Acta 707 (2011) 191–196.
[33] S. Perrier, P. Bouilloud, G. De Oliveira Coelho, M. Henry, E. Peyrin, Biosens. Bioelectron. 82 (2016) 155–161.
[34] Y. Huang, S. Zhao, Z.F. Chen, Y.C. Liu, H. Liang, Chem. Commun. 47 (2011) 4763–4765.
[35] N. Mohanty, V. Berry, Nano Lett. 8 (2008) 4469–4476.
[36] F. Kim, L.J. Cote, J. Huang, Adv. Mater. 22 (2010) 1954–1958.
[37] Y. Hu, F. Li, D. Han, et al., Anal. Chim. Acta. 753 (2012) 82–89.
[38] Y. Piao, F. Liu, T.S. Seo, Chem. Commun. 47 (2011) 12149–12151.
[39] T. Miyahata, Y. Kitamura, A. Futamura, et al., Chem. Commun. 49 (2013) 10139–10141.
[40] L. Gao, C. Lian, Y. Zhou, et al., Biosens. Bioelectron. 60 (2014) 22–29.
[41] Q. Tang, Q. Zhang, Y. Jiang, et al., ACS Appl. Mater. Inter. 6 (2014) 13470–13477.
[42] A.E. Prigodich, O.S. Lee, W.L. Daniel, et al., J. Am. Chem. Soc. 132 (2010) 10638–10641.
[43] Y. Chen, D. Tyagi, M. Lyu, et al., Anal. Chem. 91 (2019) 4017–4022.
[44] G. Kang, C.A.H. Allard, W.A. Valencia-Montoya, et al., Nature 616 (2023) 378–383.
[45] J.H. Choi, M. Shin, L. Yang, et al., ACS Nano 15 (2021) 13475–13485.
[46] Y. Liang, W.L. Ang, R.R.X. Lim, A. Bonanni, Chem. Commun. 58 (2022) 2662–2665.
[47] K. Ma, W. Xie, W. Liu, et al., Adv. Funct. Mater. 31 (2021) 2102645.
[48] J. Vilcapoma, A. Patel, A.R. Chandrasekara, K. Halvorsen, Chem. Commun. 59 (2023) 5083–5085.
[49] Y.Z. Guo, J.L. Liu, Y.F. Chen, et al., Anal. Chem. 94 (2022) 7601–7608.
[50] S. Pfister, J. Rabl, T. Wiegand, et al., Nat. Commun. 14 (2023) 1574.
[51] J. Su, W. Liu, S. Chen, et al., ACS Sens. 5 (2020) 3979–3987.